become undefined, but by setting $\eta = 0$ the pressure P becomes $\cos^{-1}(1/m\beta)$ for supersonic leading edges and $\sqrt{1/m\beta}$ for subsonic leading edges and is not a function of ξ.

This method was programmed in the FORTRAN IV language and the results obtained on a CYBER 175 computer. Since computer time varies as the size of the pressure mesh defined, it became more cost effective to trade accuracy of the results with the number of mesh points. A mesh size of 50 intervals in η and 50 intervals in ξ was found to provide sufficient accuracy for engineering purposes.

III. Results of the Method

In order to provide results useful for a large variety of configurations, the results were normalized in the same manner as was done by Pitts et al. Typical results are shown in Figs. 3 and 4. Afterbody length is presented as the fraction $\Delta X/(\beta d)$, where $\Delta X/(\beta/d) = 0$ is the no afterbody case and $\Delta X/(\beta d) = 1$ is the infinite, or full, afterbody case. The results are identical to the previously published results. For some afterbody lengths an increase in carry-over lift of up to 20% over that obtained from linear interpolation between the no-afterbody and full-afterbody cases is realized.

IV. Method Extension

Since the afterbody length is arbitrary, there seems to be no difficulty in integrating the pressure field for those bodies whose base is forward of the trailing edge of the exposed root chord, for example a wing cantilevered off of the body trailing edge. These integrations have been performed and may prove useful to some specialized configurations. The limit of the method is when $\Delta X = -C_r$.

V. Conclusion

A method has been presented which evaluates the additional lift on a cylindrical body due to a lifting surface, which accounts for the effect of finite afterbodies. Extension of the method to cantilevered surfaces is also possible. Use of the method is limited within the constraints of slender-body theory and the assumptions inherent in the formulation of Pitts et al.

References

[1] Pitts, W. C., Nielsen, J. N., and Kaattari, G. E., "Lift and Center of Pressure of Wing-Body-Tail Combinations at Subsonic, Transonic, and Supersonic Speeds," NACA 1307, 1957.

[2] Nielsen, J. N., *Missile Aerodynamics*, McGraw-Hill, New York, 1960.

AIAA 81-4114

Column Creep Buckling with End Restraint

Robert L. Carlson*
Georgia Institute of Technology, Atlanta, Ga.
and
Andrew G. Morgan Jr.†
Delta Airlines, Atlanta, Ga.

Introduction

THE problem of time-dependent buckling due to creep was first recognized in 1946 by Ross.[1] The main features of results of subsequent studies are summarized in a survey article by Hoff[2] and in a book by Hult.[3] In these studies the model analyzed is a column with hinged ends, and a variety of constitutive laws are used. For a linear-viscoelastic material column, deflection tends to infinity as time goes to infinity. If either a nonlinear time-dependent or nonlinear time-independent component of strain is present, a finite critical time is observed, and the load capacity of the column tends to zero with increasing deflection.

Recently, Huang[4] observed that the small deflection limitation used in previous analyses is not consistent with the fact that very large deflections develop as the critical time is approached. By performing a large deflection analysis, Huang[4] showed that finite critical times occur only if a lower bound load is exceeded. The nonlinear properties of constitutive laws lead to softening effects which produce the feature of finite critical time. Huang introduces geometrical nonlinearities that produce a stiffening effect which can effectively result in either longer critical times or no finite critical time.

Structural systems usually consist of many elements, and they are not free to move independently. The interactions between members are restraints of a geometric character which can further modify behavior. One form of restraint is illustrated by the column shown in Fig. 1. Clearly, the axial restraint introduced by the spring will cause a redistribution of the applied load. As the column-end displacement increases, the force in the spring increases and the force acting on the column decreases. The objective of this Note is to describe the features of this redistribution process.

Analysis

The column shown in Fig. 1 has an initial imperfection of $\bar{v}_0$, which is a function of position $\bar{x}$. The column has a two flange cross-section with each flange having an area of $A/2$ and a flange separation of h. The end restraint is represented here by a linear elastic spring.

The constitutive equations for the flanges are

$$\dot{\epsilon}_c = \frac{\dot{\sigma}_c}{E} + \left(\frac{\sigma_c}{B}\right)^m \tag{1}$$

$$\dot{\epsilon}_t = \frac{\dot{\sigma}_t}{E} + \left(\frac{\sigma_t}{B}\right)^m \tag{2}$$

where ϵ and σ are strain and stress, respectively, and the dot indicates differentiation with respect to time. The subscripts c and t refer to the concave and convex flanges. Young's modulus is E, and B and m are constants for the creep-strain rate component.

The flange stresses can be computed in terms of the nondimensional deflection $v = 2\bar{v}/h$ as

$$\sigma_c = -P/A(1+v+v_0) \tag{3}$$

$$\sigma_t = -P/A(1-v-v_0) \tag{4}$$

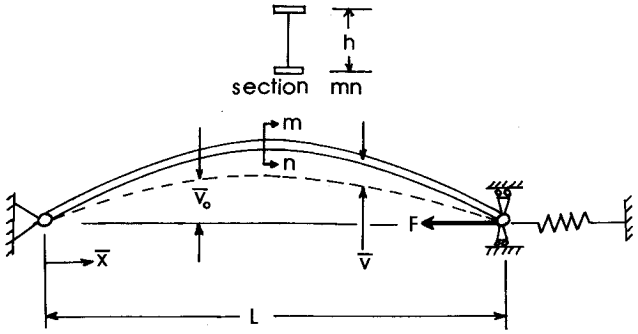

Fig. 1 Column model.

Received Sept. 4, 1980; revision received Nov. 17, 1980.

*Professor, School of Aerospace Engineering. Associate Fellow AIAA.

†Aircraft Performance Engineer, Engineering Department. Member AIAA.

where P is the time-dependent compressive force on the column.

From force equilibrium on the top hinge,

$$P=F-kd \tag{5}$$

where F is the applied force, d is the axial displacement of the hinge, and k is the spring constant.

If the effect of end restraint is confined to a consideration of moderately large deflections, a linear-strain rate vs curvature rate of change can be used:

$$\dot{\epsilon}_t-\dot{\epsilon}_c=-\frac{l}{2}\left(\frac{h}{L}\right)^2\frac{\mathrm{d}^2\dot{v}}{\mathrm{d}x^2} \tag{6}$$

where $x=\bar{x}/L$.

The end displacement can be expressed in terms of the deflection as

$$d=\frac{h^2}{8L}\int_0^l\left[\left(\frac{\mathrm{d}v}{\mathrm{d}x}\right)^2+2\frac{\mathrm{d}v}{\mathrm{d}x}\frac{\mathrm{d}v_0}{\mathrm{d}x}\right]\mathrm{d}x \tag{7}$$

Substituting Eqs. (3) and (4) in Eqs. (1) and (2), and using the results in Eq. (6) gives

$$\frac{l}{EA}\left\{-\dot{P}[(l-v-v_0)-(l+v+v_0)]+2P\dot{v}\right\}$$
$$-\left(\frac{P}{AB}\right)^m[(l-v-v_0)^m-(l+v+v_0)^m]$$
$$=-\frac{l}{2}\left(\frac{h}{L}\right)^2\frac{\mathrm{d}^2\dot{v}}{\mathrm{d}x^2} \tag{8}$$

Then, the column load can be written as

$$P=F-\frac{kh^2}{8L}\int_0^l\left[\left(\frac{\mathrm{d}v}{\mathrm{d}x}\right)^2+2\frac{\mathrm{d}v}{\mathrm{d}x}\frac{\mathrm{d}v_0}{\mathrm{d}x}\right]\mathrm{d}x \tag{9}$$

and the column load rate is

$$\dot{P}=-\frac{kh^2}{4L}\int_0^l\left(\frac{\mathrm{d}v}{\mathrm{d}x}+\frac{\mathrm{d}v_0}{\mathrm{d}x}\right)\frac{\mathrm{d}\dot{v}}{\mathrm{d}x}\,\mathrm{d}x \tag{10}$$

The use of Eqs. (9) and (10) in Eq. (8) provides a description of the deflection of the column model under the applied force F. The resulting equation is quite complex, but the features of the problem can be examined by use of a collocation method described in the paper by Hoff.[2]

Let the imperfection function be $v_0=a_0\sin\pi x$. Then, for a one term collocation solution take $v=a\sin\pi x$, which satisfies all of the boundary conditions for hinged ends. Using these functions, and collocating at $x=1/2$ gives

$$\frac{l}{EA}\left[2\dot{P}(a+a_0)+2P\dot{a}\right]-\left(\frac{P}{AB}\right)^m\left[(l-a-a_0)^m-(l+a+a_0)^m\right]=\frac{\pi^2}{2}\left(\frac{h}{L}\right)^2\dot{a} \tag{11}$$

where

$$P=F-\frac{\pi^2kh^2}{16L}a(a+2a_0) \tag{12}$$

and

$$\dot{P}=-\frac{\pi^2kh^2}{8L}\dot{a}(a+a_0) \tag{13}$$

Equations (11) and (12) can be written in the following form which is convenient for integration:

$$\int_{a(0)}^{a(t)}\frac{F(a)}{G(a)}\,\mathrm{d}a=t \tag{14}$$

where

$$F(a)=-\frac{l}{EA}\left[\frac{\pi^2kh^2}{4L}(a+a_0)^2+2P\right]-\frac{\pi^2}{2}\left(\frac{h}{L}\right)^2 \tag{15}$$

and

$$G(a)=\left[\frac{F}{AB}-\frac{\pi^2kh^2}{16ABL}a(a+2a_0)\right]^m$$
$$\times[(l-a-a_0)^m-(l+a+a_0)^m] \tag{16}$$

Numerical Results

The geometric values used in an example computation are $L=0.2761$ m (0.9058 ft), $h=5.08\times10^{-3}$ m (0.0167 ft), $A=77.41\times10^{-6}$ m^2 (0.8332×10^{-3} ft^2), and $a_0=0.1$. The material property constants used are those given by Hult[3] for a carbon steel at 500°C, and they are $E=167\times10^3$ MN/m^2 (24.2×10^6 psi), $B=10^5$ MN/m^2 s$^{1/3}$ (1.45×10^7 psi s$^{1/3}$), and $m=3$. Finally, the applied force F is 77.41×10^{-4} MN (17.40×10^2 lb).

Equation (14) is numerically integrated by the use of Simpson's rule for two cases: $k=0$ and $k=4$ MN/m (0.2741×10^6 lb/ft). The deflection histories are plotted as solid curves in Fig. 2. For $k=0$, the critical time is 28 h. For $k=4$ MN/m, the stabilizing effect of the spring is apparent. Also shown in Fig. 2 as dashed curves are the column force histories. Without the spring, the column force remains constant. With an end spring, the force decreases continuously and causes a decreasing column deflection rate.

The form of the deflection curve for $k=4$ MN/m suggests the possibility that the deflection rate $\dot{a}$ might go to zero. To study this behavior, it is useful to rewrite Eq. (14) as a differential equation of the form

$$\dot{a}=G(a)/F(a) \tag{17}$$

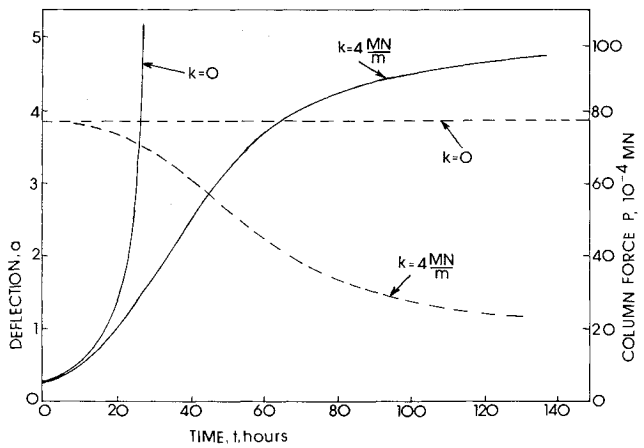

Fig. 2 Deflection and column force histories.

An examination of the ratio in Eq. (17) indicates that if either $F\to\infty$ or $G\to 0$, then $\dot{a}\to 0$. The first alternative is not possible, but the second is. Thus, the condition for $\dot{a}=0$ can be taken to be $G(a)=0$. Examination of Eq. (16) indicates that this condition leads to the requirement that

$$F=\frac{\pi^2 kh^2}{16L}a(a+2a_0) \tag{18}$$

Thus, the combinations of values of F, a, k, and a_0 for which $\dot{a}\to 0$ can be determined.

Discussion

Nonlinear constitutive laws produce softening effects which lead to finite collapse times in column creep. If nonlinear geometrical effects are included in the analysis, collapse times are either increased or eliminated. Two geometrical effects which can produce stiffening are the nonlinear strain-curvature relation studied by Huang[4] and the end restraint effect examined in this Note.

Finally, it should be noted that although the stabilizing influence of nonlinear geometric effects might alleviate a concern for collapse, Böstrom[5] indicates that another failure mode should also be considered. He showed that when creep-induced embrittlement processes are operative, fracture may be the mode of failure. Creep buckling experiments on polypropylene plastic columns at room temperature have, in fact, been observed to terminate ultimately by fracture.[6] Because many heat resistant alloys are subject to embrittlement, the fracture mode of failure should be considered a distinct possibility.

References

[1]Ross, A. D., "The Effects of Creep on Instability and Indeterminacy Investigated by Plastic Models," *The Structural Engineer,* Vol. 24, No. 8, Aug. 1946, p. 413.

[2]Hoff, N. J., "A Survey of the Theories of Creep Buckling," *Proceedings of the Third U. S. National Congress of Applied Mechanics,* ASME, 1958, pp. 29-49.

[3]Hult, J., *Creep in Engineering Structures,* Blaisdell Publishing Co., Waltham, Mass., 1966, pp. 61-71.

[4]Huang, N. C., "Creep Buckling of Imperfect Columns," *Journal of Applied Mechanics,* March 1976, pp. 131-136.

[5]Böstrom, P. O., "Creep Buckling Considering Material Damage," *International Journal of Solids and Structures,* Vol. 11, June 1975, pp. 765-775.

[6]Morgan, A. G. Jr., "Column Creep Buckling With Elastic End Restraint," Special Problem Submitted to School of Aerospace Engineering, Georgia Institute of Technology, April 1980.

AIAA 81-4115

Effective Radiation Scattering Coefficient

D. C. Look Jr.*
University of Missouri-Rolla, Rolla, Mo.

Nomenclature

c' = effective scattering coefficient, $=C_{sca}/V_p$
C_{sca} = scattering cross section
D = scattering particle diameter; particle is a sphere
I = intensity
ℓ = path length
N_0 = particle number density
n = relative index of refraction
T = transmittance
V_p = scattering particle volume, $=\pi D^3/6$
x = size parameter, $n_w\pi D/\lambda_0$; n_w is water refractive index
η = particle volume concentration
λ_0 = wavelength in vacuum, 0.6328 μm
τ = optical thickness, $=N_0C_{sca}\ell$

Introduction

In previously reported work[1-3] an effective scattering coefficient c' was presented. This coefficient, although convenient from an experimental point of view, may be a bit unusual since it is the ratio of scattering cross section C_{sca} and the scattering particle volume V_p. The purpose of this Note is to present the variation of this coefficient as a function of particle size assuming a purely scattering media. Once obtained, this coefficient could then be used to determine the scattering cross section. Instead, in this presentation, the values of the theoretical and experimental effective scattering coefficient as a function of scattering particle diameter are compared in both tabular and graphical forms.

Discussion

Transmission data have been obtained for an assumed purely scattering media using 11 sets of uniformally sized polystyrene latex spheres as scattering centers. The latex spheres were diluted with distilled water to produce solutions of known concentrations. Transmission measurements of these concentrations at one wavelength (0.6328 μm) were then obtained. The spectrophotometer used had a path length of 1 cm and measured the transmission relative to another cell containing distilled water only.

The transmission of a scattering media is a function of the scattering sphere number density N_0, the scattering cross section C_{sca}, and path length ℓ

$$T=\exp(-\tau)=\exp(-N_0C_{sca}\ell) \tag{1}$$

The scattering medium was characterized by the scattering spheres volume concentration η, which is the ratio of the volume of scattering spheres and volume of the scattering spheres plus the volume of distilled water that is added to dilute the suspension. The number density of spheres in a unit volume of concentration η is $N_0=\eta/V_p$, where V_p is the volume of a single sphere, $\pi D^3/6$. Thus, the optical thickness of the purely scattering medium may be written as

$$\tau=(\eta/V_p)C_{sca}\ell=\eta c'\ell \tag{2}$$

where c', the effective scattering coefficient, equals C_{sca}/V_p and has units of cm^{-1}.

One determines c' experimentally by measuring the transmission through a cell containing distilled water and the scattering media relative to the transmission through another cell containing just distilled water. In the pure distilled water case, the power transmitted through the cell is closely approximated by the expression

$$I_w=I_0(1-\rho_1)(1-\rho_2)e^{-\tau_w} \tag{3}$$

where ρ_1 and ρ_2 are the front and back cell wall reflectances, respectively, τ_w the optical thickness of the distilled water, and I_0 the incident radiation. In the distilled water-scattering media case, the corresponding expression is

$$I_s=I_0(1-\rho_3)(1-\rho_4)e^{-\tau_w-\tau} \tag{4}$$

where ρ_3 and ρ_4 are the front and back cell wall reflectances of a second cell and are assumed to be different than ρ_1 and ρ_2 (i.e., the cells are not truly identical). τ is the optical thickness

Received Nov. 3, 1980.

*Professor, Thermal Radiative Transfer Group, Mechanical and Aerospace Engineering.